# Ion specificity at the peptide bond: Molecular dynamics simulations of N-methylacetamide in aqueous salt solutions

Jan Heyda,[1] Jordan C. Vincent,[2] Douglas J. Tobias,[2] Joachim Dzubiella,[3] and Pavel Jungwirth[1]

*[1]Institute of Organic Chemistry and Biochemistry, Academy of Sciences of the Czech Republic, and Center for Biomolecules and Complex Molecular Systems, Flemingovo nám. 2, 16610 Prague 6, Czech Republic, [2]Department of Chemistry, University of California at Irvine, Irvine CA 92697-2025, USA, [3]Department of Physics T37, Technical University Munich, 85748 Garching, Germany*

**Abstract**

Affinities of alkali cations and halide anions for the peptide group were quantified using molecular dynamics simulations of aqueous solutions of N-methylacetamide using both non-polarizable and polarizable force fields. Potassium and, more strongly, sodium exhibit an affinity for the carbonyl oxygen of the amide group, while none of the halide anions shows any appreciable attraction for the amide hydrogen. Heavier halides, however, interact with the hydrophobic methyl groups of N-methylacetamide. Using the present results for a model of the peptide bond we predict that the destabilizing effect of weakly hydrated Hofmeister ions, such as bromide or iodide, is not due to direct interactions with the backbone but rather due to attraction to hydrophobic regions of the protein.

## Introduction

Proteins can be destabilized by various chemical agents, such as urea or certain salts. Despite experimental and computational efforts the detailed molecular mechanisms of protein denaturation have not been fully established yet. Recent studies show that the most common denaturant, i.e., urea interacts primarily with the protein backbone, [1-4] although contacts with non-polar (particularly aromatic) side chains have been also found to be important.[5-11] However, the interaction between urea and the protein amide bond is not much stronger than that of water, which further complicates nailing down the denaturating mechanism. A recent spectroscopic study on a popular protein proxy, poly(*N*-isopropylacrylamide) in aqueous solutions of urea, indicates that the effect on protein folding and unfolding may be rather indirect and potentially also connected with entropic factors due to diferent sizes of urea and water molecules.[4]

Of denaturating salts, guanidinium chloride has been shown to be particularly efficient despite the fact that guanidinium does not seem to be strongly interacting with the protein backbone.[2] Guanidinium rather exhibits affinity for amino acid side chains, in particular aromatic ones.[12] Similar, albeit weaker destabilization of proteins is also caused by other ions such as large soft inorganic anions. An important question thus arises as to how common salts in water interact with the protein backbone[13,14] and whether contacts with the amide group are related to the denaturating ability of weakly hydrated ions in the Hofmeister series,[15,16] such as heavier halides, thiocyanate, perchlorate, etc.

N-methylacetamide (NMA) is one of the simplest molecules containing the amide group and has, therefore, been employed as a suitable model for studying interactions at the protein backbone.[17-20] On one hand, extensive MD simulations have been performed in order to characterize pure liquid NMA[21,22] and aqueous NMA solutions.[19] The latter have been also complemented by integral equation theory[23] and NMR experiments.[24] On the other

hand, interactions between NMA and selected inorganic ions such as alkali cations have been characterized in the gas phase[25-27] and in small water clusters.[20] The purpose of the present study is to fill the existing gap by simulating NMA in bulk aqueous solutions of alkali halides. By performing an extensive series of molecular dynamics (MD) simulations we attempt to address the question concerning interactions of common ions such as alkali cations and halide anions with the amide bond and their potential consequences for mechanisms of protein denaturation by chemical agents.

**Systems and Methods**

We performed MD simulations of NMA as a proxy to the amide bond in proteins in aqueous alkali halide solutions. In particular, we simulated 1 M of NMA in 1 M solutions of NaCl, KCl, KBr, NaBr, and mixed solutions thereof. Additionally, we also simulated a single NMA in 1 M aqueous solutions of KF or NaI. To further check concentration effects, we did also test simulations of a single molecule of NMA in 0.5 M salt solutions.

Both non-polarizable and polarizable force fields were employed in the present simulations. For NMA, the parm99 potential (without or with polarizability) was used with the molecule constructed from ACE and NME residues.[28] This potential, which is rather similar to those employed for NMA previously,[19,21,22,29] utilizes the same Lennard-Jones parameters as are used for the amide bond in proteins within the parm99 force field. For comparison, we also performed test simulations with a non-polarizable parm99 force field for the NMA molecule, which has slightly different partial charges and Lennard-Jones parameters.[28] This did not change the binding patterns of alkali cations and halide anions to NMA in water. Quantitatively, the only notable difference was the reduction of the preference of $Na^+$ over $K^+$ for NMA, which can be traced primarily to increased van der Waals radius of the carbonyl oxygen in this parameterization.

For water, we employed either the non-polarizable SPCE[30] or polarizable POL3[31] models. For sodium, potassium, chloride, and bromide we used practically the same parameters (without or with polarizability) as in our previous studies of ions in water.[32,33] For comparison and consistency check we additionally performed simulations using other popular ion force fields[34,35] in combination with the TIP3P water model.[36] For reference, all employed ionic parameters with corresponding references are summarized in Table 1.

The total simulation time for each run was 100 ns (after equilibration of 1 ns) with a time step of 1 fs. The coordinates were saved every 1 ps yielding 100 000 frames for further analysis. By dividing this set of frames to 2-5 parts we checked that the simulation length was long enough to provide converged results. For the 1 M NMA in 1 M alkali halide solution the unit cell of 26.3×26.3×26.3 Å contained approximately 400 water molecules, 8 NMA molecules, 8 cations and 8 anions. 3D periodic boundary conditions were applied with long range electrostatic interactions beyond the non-bonded cutoff of 9 Å accounted for using the Particle Mesh Ewald (PME) method.[37] The Berendsen temperature ( 300 K) and pressure (1 atm) couplings were used[38] and all bonds containing hydrogen were constrained using the SHAKE algorithm.[39]

The simulated trajectories were analyzed primarily in terms of radial distribution functions (RDF) and their integrals which provide the total number of the other species within a given distance from the investigated moiety. In particular, we have evaluated the alkali cation-oxygen of the amide, halide anion-hydrogen of the amide, halide anion-methyl carbons, alkali cation-halide anion, and ion-water distributions, averaged over the production part of each trajectory. All MD simulations were performed using the Amber 10 program.[40]

**Results**

Figures 1 and 2 shows radial distribution functions and integrals thereof between an alkali cation (sodium or potassium) and the electronegative carbonyl oxygen of the amide group, as obtained from MD simulations of 1 M of NMA in aqueous solutions of NaCl, KCl, NaBr, KBr, and NaCl/KBr mixture, all with salt concentration of 1 M. The prinicipal result is that both cations exhibit an appreciable affinity for the carbonyl oxygen, as demonstrated by strong peaks at the RDFs corresponing to carbonyl oxygen-alkali cation contact pairs. This affinity is significantly stronger for $Na^+$ than $K^+$ as reflected in the integral curves, which provide the numbers of cations within a given distance from the carbonyl oxygen. Moreover, sodium wins over potassium both for contact and solvent-separated ion pairs, as is clear from the relative ($Na^+$ vs $K^+$) heights of the first two RDF peaks and, particularly, from the fact that the plateau of the integral curve around 3.5 Å is higher for sodium than for potassium and the difference between the two curves further increases up to about 5 Å. These observations are robust with respect to change of a force field from a non-polarizable (Figure 1) to a polarizable (Figure 2) model. Upon moving from single salt to mixed solutions the relative preference of the carbonyl oxygen of the amide group for sodium over potassium persists and, particularly for the non-polarizable simulations, even becomes stronger. This points to a certain degree of competition between $Na^+$ and $K^+$ for the binding site at NMA, in which the former cation is a clear winner over the latter.

The fact that sodium binds more strongly to the carbonyl oxygen of the amide bond than potassium reflects itself not only in structural observables like RDFs but also in time-dependent properties such as the mean residence times of the ions in the vicinity of NMA. Figure 3 shows the distribution of contact times of $Na^+$ and $K^+$ with the carbonyl oxygen, as extracted from the non-polarizable or polarizable simulation. To construct these distributions, we have followed all contact pairs between the carbonyl oxygen of NMA and an alkali cation

(with separation smaller than 3.5 Å) transiently formed (for more than 5 ps) during the simulations and histogramed their durations. Consistently for both force fields the contacs with sodium are on average about three times longer than those with potassium (residence times from exponential fits of ~37 vs ~12 ps, respectively).

The interaction of the alkali cations with water molecules is practically unaffected by the chemical nature of the halide counter-anion, at least at the 1 M concentration investigated here. This is demonstrated in Figure 4, which shows little change in sodium-water oxygen and potassium-water oxygen RDFs upon moving from single salt to mixed solutions, both in non-polarizable and polarizable simulations. At a concentration of 1 M, pairing between alkali cations and halide anions is already non-negligible. Figures 5 and 6 show the cation-anion RDFs for non-polarizable and polarizable simulations. One can see, that potassium pairs more strongly than sodium with heavier halides (chloride and, in particular, bromide) with the effect of salt mixing being very small. Also, the influence of adding polarization is rather modest.

Figures 7 and 8 show the interaction between halide anions and the electropositive amide hydrogen in NMA. Unlike the alkali cations, chloride and bromide do not exhibit an appreciable affinity for the amide group, neither in non-polarizable nor in polarizable simulations, the results of which are very similar to each other. For $Cl^-$ the first peak at the RDF does not even cross unity (which corresponds to average bulk concentration) while it only barely does so for $Br^-$. Another potential site for attraction of heavier halides are the methyl groups in NMA. While alkali cations are repelled from such hydrophobic groups, bromide and, to a lesser extent, also chloride exhibit an affinity for them, particularly in the polarizable calculations (Figures 9 and 10). Including polarization, the attraction of halides for the methyl groups becomes stronger and is now for both $Cl^-$ and $Br^-$ more significant that for the amide group. Like in the case of alkali cations, the water solvent shell around chloride

and bromide is practically unaffected by moving from single salt to a mixed solution (Figure 11). However, changing the force field from non-polarizable to polarizable slightly reduces the water density around the anions.

We have also investigated the possibility of pairing and aggregation of NMA molecules themselves in the aqeuous salt solutions. The RDFs between amide hydrogen on one NMA and carbonyl oxygen of another NMA exhibit a weak tendency for pairing by forming intermolecular hydrogen bonds at the 1 M concentration of NMA, both in non-polarizable and polarizable simulations (Figure 12). Nevertheless, to check the effect of this weak pairing on interactions with ions we have performed a very long simulation of just a single NMA molecule in a mixed NaCl/KCl solution of a total concentration of 1 M. The resulting alkali cation-carbonyl oxgen RDFs are very similar to those for 1 M NMA, indicating that the observed weak association of NMA molecules practically does not affect their interaction with dissolved ions.

The lack of appreciable affinity of chloride and bromide for the amide bond raises the question whether halides that lie further from the center of the Hofmeister series, i.e., fluoride on one side and iodide on the other side, could not interact more strongly. To address this question, we have performed additional polarizable simulations of 1 M NMA in 1 M KF or NaI solutions. The resulting halide anion-amide hydrogen RDFs depicted in Figure 13 demonstrate that even these “extreme” halides in the periodic table are no more attracted to the amide bond than chloride and bromide. Also, the presence of flouride or iodide as counter-ions does not change the relative affinities of sodium vs potassium for the carbonyl oxygen in the amide bond. This follows from Figure 14 which compares the alkali cation-carbonyl oxygen RDFs in 1 M KF and NaI solutions. However, iodide does adsorb much more strongly to the hydrophobic groups of NMA than lighter halides, as demonstrated on the right panel of

Figure 13 showing a strong peak on the iodide–methyl carbon RDF and the lack thereof for fluoride.

In order to further check the robustness of the present results with respect to the interaction potential, we have repeated the simulations of 1 M NMA in a mixed NaCl/KBr aqueous solution employing a somewhat different non-polarizable force field for the ions than used above (see Table I). The resulting ion-NMA affinities are in a quantitative agreement with the above results, as demonstrated by the alkali cation-carbonyl oxygen RDFs depicted in Figure 15.

**Discussion**

Alkali cations exhibit an appreciable affinity and selectivity at the carbonyl oxygen of the peptide bond of NMA. This attraction and preference of sodium over potassium is in accord with our previous observations of interactions of $Na^+$ and $K^+$ with surfaces of various proteins.[41] It is also consistent with analysis of amide solubility data using a thermodynamic partitioning model.[42] It is remarkable that the relative preference of sodium over potassium at the peptide bond is qualitatively the same as (albeit weaker than) that at the negatively charged carboxylate side chains of Glu and Asp. In other words, these two regions on protein surfaces work in concert in attracting and differentiating between alkali cations.

The present observation of the lack of appreciable affinity of any of the halide anions for the amide hydrogen in NMA is surprising in the light of a generally stronger effect of anions vs cations on protein stability. Our results indicate that, unlike urea, destabilizing anions such as bromide and iodide interact more strongly with hydrophobic moieties than with the peptide bond. Therefore, the molecular mechanism of protein destabilization and denaturation by ions may be different from that of the neutral urea molecule and may involve solubilization of hydrophobic regions of proteins by adsorption of large polarizable (soft)

ions. A high affinity of iodide to non-polar side chains has indeed been found to be a key component of denaturation of a α-helical peptide in a recent simulation study of one of the present authors.[43] Our findings are also consistent with earlier experiments emphasizing the importance of the non-polar methyl groups for the halide anion-NMA interactions[17] and with the predictions from the thermodynamic partitioning model.[42]

The observed affinity of alkali cations to the peptide bond and lack thereof for halide anions is robustly predicted from both non-polarizable and polarizable MD simulations, with the ion-amide RDFs being very similar to each other for the two force fields. The robustness of the results was also checked by switching between two somewhat different non-polarizable force fields for ions. The only observable that was found to change significantly (i.e., increase) with the addition of polarization is the affinity of larger anions for hydrophobic methyl groups of NMA. This is yet another demonstration of the importance of polarization effects for segregation of ions at hydrophobic aqueous interfaces.[44] Finally, the observed trends in the relative strength of interactions of alkali cations and halide anions with the peptide bond in NMA depend only weakly on the particular counter-ion and concentration of salt or NMA.

**Conclusions**

Using MD simulations of 100 ns duration we have obtained converged RDFs between alkali cations/halide anions and the amide bond of NMA in aqueous solutions. Using both non-polarizable and polarizable force fields we have robustly shown that alkali cations show an appreciable affinity for the amide bond while the halide anions don't. Between sodium and potassium the former is the winner in terms of attraction for the carbonyl oxygen of NMA and this cation specificity is qualitatively the same as that at the carboxylate group of negatively charged amino acids Glu and Asp. The only appreciable interaction with NMA observed for

anions was that of heavier halides with the hydrophobic methyl groups, particularly in the polarizable simulations.

Despite the fact that NMA is only a model for the peptide bond and the actual situation in proteins is much more complex we can conclude, based on the present results, that weakly hydrated Hofmeister anions (such as bromide or iodide) probably do not destabilize proteins via direct interactions with the backbone amide groups. We rather suggest that this destabilizing activity may be partly due to the affinity of large soft ions for hydrophobic groups and residues, which makes them more accessible to the aqueous solvent.

**Acknowledgement**

We thank the Czech Science Foundation (grants 203/08/0114) and the Czech Ministry of Education (grant LC512) and for support**.** We also acknowledge support from AirUCI, which is funded by the National Science Foundation (grants CHE-0431312 and CHE-0209719). JH thanks the International Max-Planck Research School for support. The Institute of Organic Chemistry and Biochemistry is supported by Project Z4 055 0506. JD is grateful to the Deutsche Forschungsgemeinschaft (DFG) for support within the Emmy-Noether-Program and the Leibniz Rechenzentrum (LRZ) München for computing time on HLRB II.

**References**

(1) Street, T. O.; Bolen, D. W.; Rose, G. D. *Proceedings of the National Academy of Sciences of the United States of America* **2006**, *103*, 17064.

(2) Lim, W. K.; Rosgen, J.; Englandera, S. W. *Proceedings of the National Academy of Sciences of the United States of America* **2009**, *106*, 2595.

(3) Auton, M.; Holthauzen, L. M. F.; Bolen, D. W. *Proceedings of the National Academy of Sciences of the United States of America* **2007**, *104*, 15317.

(4) Sagle, L. B.; Zhang, Y. J.; Litosh, V. A.; Chen, X.; Cho, Y.; Cremer, P. S. *Journal of the American Chemical Society* **2009**, *131*, 9304.

(5) Baldwin, R. L. *Biophysical Journal* **1996**, *71*, 2056.

(6) Goette, M.; Stumpe, M. C.; Ficner, R.; Grubmuller, H. *Biophysical Journal* **2009**, *97*, 581.

(7) Stumpe, M. C.; Grubmuller, H. *Biophysical Journal* **2009**, *96*, 3744.

(8) Stumpe, M. C.; Grubmuller, H. *Journal of the American Chemical Society* **2007**, *129*, 16126.

(9) Canchi, D. R.; Paschek, D.; Garcia, A. E., submitted.

(10) Hua, L.; Zhou, R. H.; Thirumalai, D.; Berne, B. J. *Proceedings of the National Academy of Sciences of the United States of America* **2008**, *105*, 16928.

(11) Das, A.; Mukhopadhyay, C. *Journal of Physical Chemistry B* **2009**, DOI: 10.1021/jp903554n.

(12) Mason, P. E.; Brady, J. W.; Neilson, G. W.; Dempsey, C. E. *Biophysical Journal* **2007**, *93*, L4.

(13) Sedlak, E.; Stagg, L.; Wittung-Stafshede, P. *Archives of Biochemistry and Biophysics* **2008**, *479*, 69.

(14) Vaney, M. C.; Broutin, I.; Retailleau, P.; Douangamath, A.; Lafont, S.; Hamiaux, C.; Prange, T.; Ducruix, A.; Ries-Kautt, M. *Acta Crystallographica Section D-Biological Crystallography* **2001**, *57*, 929.

(15) Kunz, W.; Henle, J.; Ninham, B. W. *Current Opinion in Colloid & Interface Science* **2004**, *9*, 19.

(16) Zhang, Y. J.; Cremer, P. S. *Current Opinion in Chemical Biology* **2006**, *10*, 658.

(17) Nandi, P. K.; Robinson, D. R. *Journal of the American Chemical Society* **1972**, *94*, 1299.

(18) Schrier, E. E.; Schrier, E. B. *Journal of Physical Chemistry* **1967**, *71*, 1851.

(19) Allison, S. K.; Bates, S. P.; Crain, J.; Martyna, G. J. *Journal of Physical Chemistry B* **2006**, *110*, 21319.

(20) Miller, D. J.; Lisy, J. M. *Journal of Physical Chemistry A* **2007**, *111*, 12409.

(21) Whitfield, T. W.; Martyna, G. J.; Allison, S.; Bates, S. P.; Crain, J. *Chemical Physics Letters* **2005**, *414*, 210.

(22) Whitfield, T. W.; Martyna, G. J.; Allison, S.; Bates, S. P.; Vass, H.; Crain, J. *Journal of Physical Chemistry B* **2006**, *110*, 3624.

(23) Beglov, D.; Roux, B. *Journal of Chemical Physics* **1996**, *104*, 8678.

(24) Hinton, J. F.; Amis, E. S.; Mettetal, W. *Spectrochimica Acta Part a-Molecular Spectroscopy* **1969**, *A 25*, 119.

(25) Tsang, Y.; Siu, F. M.; Ho, C. S.; Ma, N. L.; Tsang, C. W. *Rapid Communications in Mass Spectrometry* **2004**, *18*, 345.

(26) Klassen, J. S.; Anderson, S. G.; Blades, A. T.; Kebarle, P. *Journal of Physical Chemistry* **1996**, *100*, 14218.

(27) Roux, B.; Karplus, M. *Journal of Computational Chemistry* **1995**, *16*, 690.

(28) Wang, J. M.; Wolf, R. M.; Caldwell, J. W.; Kollman, P. A.; Case, D. A. *Journal of Computational Chemistry* **2004**, *25*, 1157.

(29) Walsh, T. R.; Liang, T. *Journal of Computational Chemistry* **2009**, *30*, 893.

(30) Berendsen, H. J. C.; Grigera, J. R.; Straatsma, T. P. *Journal of Physical Chemistry* **1987**, *91*, 6269.

(31) Caldwell, J. W.; Kollman, P. A. *Journal of Physical Chemistry* **1995**, *99*, 6208.

(32) Jungwirth, P.; Tobias, D. J. *Journal of Physical Chemistry B* **2001**, *105*, 10468.

(33) Wick, C. D.; Dang, L. X.; Jungwirth, P. *Journal of Chemical Physics* **2006**, *125*.

(34) Dang, L. X. *Journal of the American Chemical Society* **1995**, *117*, 6954.

(35) Koneshan, S.; Rasaiah, J. C.; Lynden-Bell, R. M.; Lee, S. H. *Journal of Physical Chemistry B* **1998**, *102*, 4193.

(36) Jorgensen, W. L.; Chandrasekhar, J.; Madura, J. D.; Impey, R. W.; Klein, M. L. *Journal of Chemical Physics* **1983**, *79*, 926.

(37) Essmann, U.; Perera, L.; Berkowitz, M. L.; Darden, T.; Lee, H.; Pedersen, L. G. *Journal of Chemical Physics* **1995**, *103*, 8577.

(38) Berendsen, H. J. C.; Postma, J. P. M.; Vangunsteren, W. F.; Dinola, A.; Haak, J. R. *Journal of Chemical Physics* **1984**, *81*, 3684.

(39) Ryckaert, J. P.; Ciccotti, G.; Berendsen, H. J. C. *Journal of Computational Physics* **1977**, *23*, 327.

(40) D.A. Case, T. A. D., T.E. Cheatham, III, C.L. Simmerling, J. Wang, R.E. Duke, R. Luo,; M. Crowley, R. C. W., W. Zhang, K.M. Merz, B.Wang, S. Hayik, A. Roitberg, G. Seabra, I.; Kolossváry, K. F. W., F. Paesani, J. Vanicek, X.Wu, S.R. Brozell, T. Steinbrecher, H. Gohlke,; L. Yang, C. T., J. Mongan, V. Hornak, G. Cui, D.H. Mathews,

M.G. Seetin, C. Sagui, V. Babin,; Kollman, P. A. *Amber 10* **2008**, University of California San Francisco.

(41) Vrbka, L.; Vondrasek, J.; Jagoda-Cwiklik, B.; Vacha, R.; Jungwirth, P. *Proceedings of the National Academy of Sciences of the United States of America* **2006**, *103*, 15440.

(42) Pegram, L. M.; Record, M. T. *Journal of Physical Chemistry B* **2008**, *112*, 9428.

(43) Dzubiella, J. *Journal of the American Chemical Society* **2008**, *130*, 14000.

(44) Jungwirth, P.; Tobias, D. J. *Chemical Reviews* **2006**, *106*, 1259.

(45) Perera, L.; Berkowitz, M. L. *Journal of Chemical Physics* **1991**, *95*, 1954.

(46) Chang, T. M.; Dang, L. X. *Journal of Physical Chemistry B* **1999**, *103*, 4714.

(47) Perera, L.; Berkowitz, M. L. *Journal of Chemical Physics* **1994**, *100*, 3085.

(48) Cabarcos, O. M.; Weinheimer, C. J.; Martinez, T. J.; Lisy, J. M. *Journal of Chemical Physics* **1999**, *110*, 9516.

(49) Markovich, G.; Perera, L.; Berkowitz, M. L.; Cheshnovsky, O. *Journal of Chemical Physics* **1996**, *105*, 2675.

**Tables:**

**Table 1** Lennard-Jones potential parameters and polarizabilities for alkali cations and halide anions employed in this study.

| **Ions** | σ [Å] | ε [kcal/mol] | α [Å$^3$] | reference. |
|---|---|---|---|---|
| $Na^+$ | 2.350 | 0.13 | 0.24 | [45] |
| $Na^+$ modified | 2.586 | 0.1 | --- | [34] |
| $K^+$ | 3.156 | 0.1 | 0.83 | [46] |
| $K^+$ modified | 3.334 | 0.1 | --- | [34] |
| $F^-$ | 3.168 | 0.2 | 0.974 | [47] |
| $Cl^-$ | 4.339 | 0.1 | 3.69 | [47,48] |
| $Cl^-$ modified | 4.401 | 0.1 | --- | [34] |
| $Br^-$ | 4.700 | 0.1 | 4.53 | [49] |
| $Br^-$ modified | 4.538 | 0.1 | --- | [35] |
| $I^-$ | 5.149 | 0.1 | 6.9 | [49] |

**Figure captions**

**Figure 1** Carbonyl oxygen – alkali cation radial distribution functions and cumulative sums in pure and mixed solutions. Results from simulations with a non-polarizable force field.

**Figure 2** Carbonyl oxygen – alkali cation radial distribution functions and cumulative sums in pure and mixed solutions. Results from simulations with a polarizable force field.

**Figure 3** Distributions of durations of contacts of transiently formed C=O...$Na^+$ and C=O...$K^+$pairs and the corresponding exponential fits. Nonpolarizable (left) and polarizable (right) force fields.

**Figure 4** Water oxygen – sodium cation (left) and water oxygen – potassium cation (right) radial distribution functions and cumulative sums in pure and mixed solutions modeled using both non-polarizable and polarizable force fields.

**Figure 5** Alkali cation – halide anion radial distribution functions and cumulative sums in pure and mixed solutions. Results from simulations with a non-polarizable force field.

**Figure 6** Alkali cation – halide anion radial distribution functions and cumulative sums in pure and mixed solutions. Results from simulations with a polarizable force field.

**Figure 7** Amide hydrogen – halide anion radial distribution functions and cumulative sums in pure and mixed solutions. Results from simulations with a non-polarizable force field.

**Figure 8** Amide hydrogen – halide anion radial distribution functions and cumulative sums in pure and mixed solutions. Results from simulations with a polarizable force field.

**Figure 9** Methyl group carbon – halide anion radial distribution functions and cumulative sums in pure and mixed solutions. Results from simulations with a non-polarizable force field.

**Figure 10** Methyl group carbon – halide anion radial distribution functions and cumulative sums in pure and mixed solutions. Results from simulations with a polarizable force field.

**Figure 11** Water oxygen – halide anion radial distribution functions and cumulative sums in pure and mixed solutions. Non-polarizable (left) and polarizable (right) force fields.

**Figure 12** Carbonyl oxygen – amide hydrogen radial distribution function. Non-polarizable (left) and polarizable (right) force fields.

**Figure 13** Amide hydrogen – fluoride or iodide (left) and methyl carbon – fluoride or iodide (right) radial distribution functions and cumulative sums in KF and NaI solutions. Results from simulations with a polarizable force field.

**Figure 14** Carbonyl oxygen – alkali cation radial distribution functions and cumulative sums in KF and NaI solutions. Results from simulations with a polarizable force field.

**Figure 15** Carbonyl oxygen – alkali cation radial distribution functions and cumulative sums in pure and mixed solutions. Results from simulations with a modified non-polarizable force field.

**Figure 1**

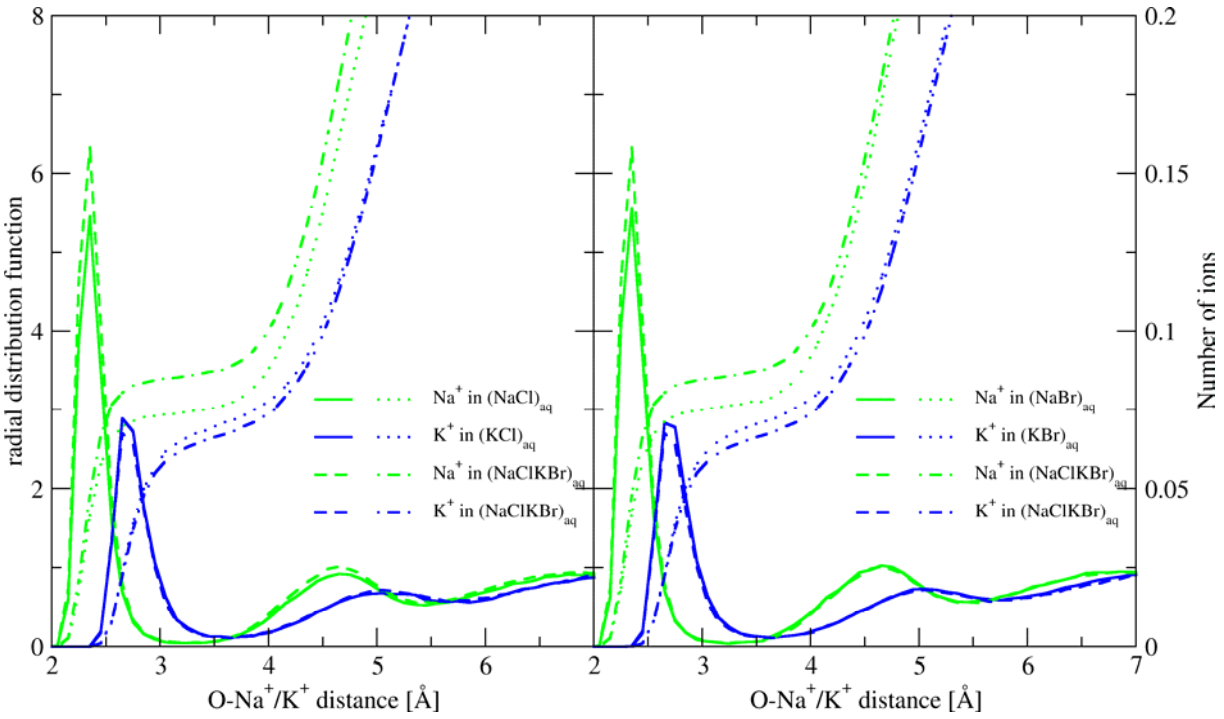
radial distribution function
Number of ions
O-Na+/K+ distance [Å]
O-Na+/K+ distance [Å]
Na+ in (NaCl)aq
K+ in (KCl)aq
Na+ in (NaClKBr)aq
K+ in (NaClKBr)aq
Na+ in (NaBr)aq
K+ in (KBr)aq
Na+ in (NaClKBr)aq
K+ in (NaClKBr)aq

**Figure 2**

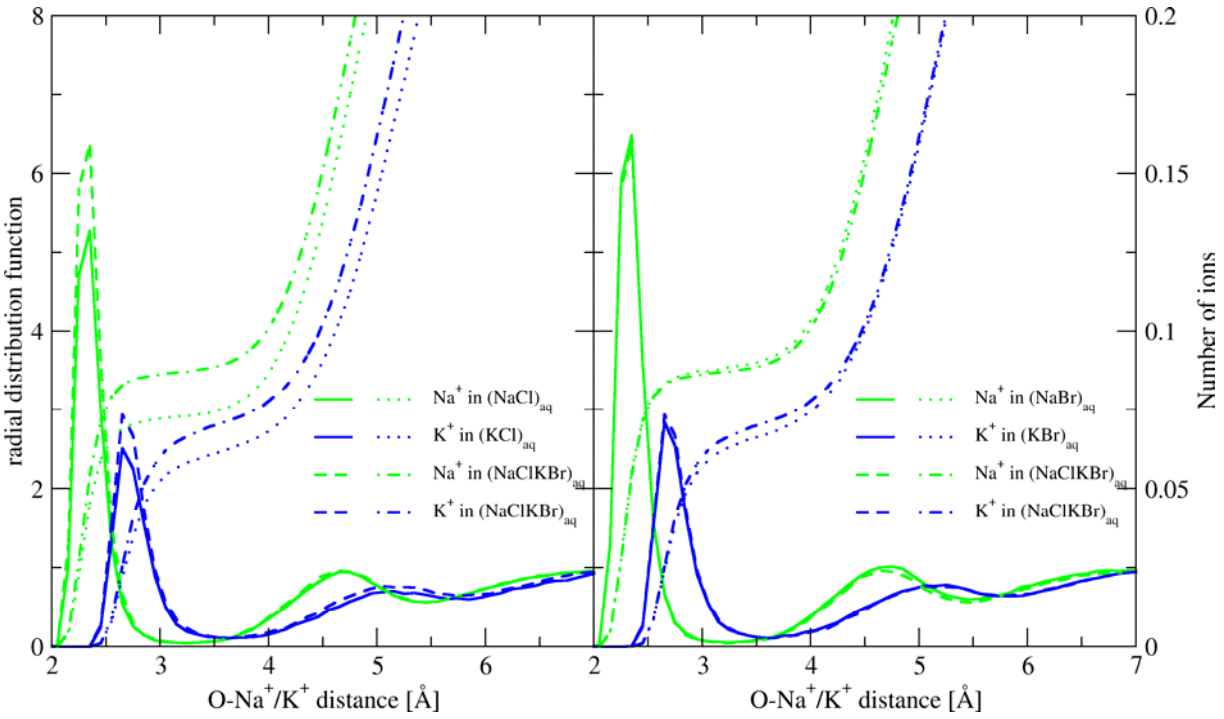
radial distribution function
Number of ions
O-Na+/K+ distance [Å]
O-Na+/K+ distance [Å]
Na+ in (NaCl)aq
K+ in (KCl)aq
Na+ in (NaClKBr)aq
K+ in (NaClKBr)aq
Na+ in (NaBr)aq
K+ in (KBr)aq
Na+ in (NaClKBr)aq
K+ in (NaClKBr)aq

**Figure 3**

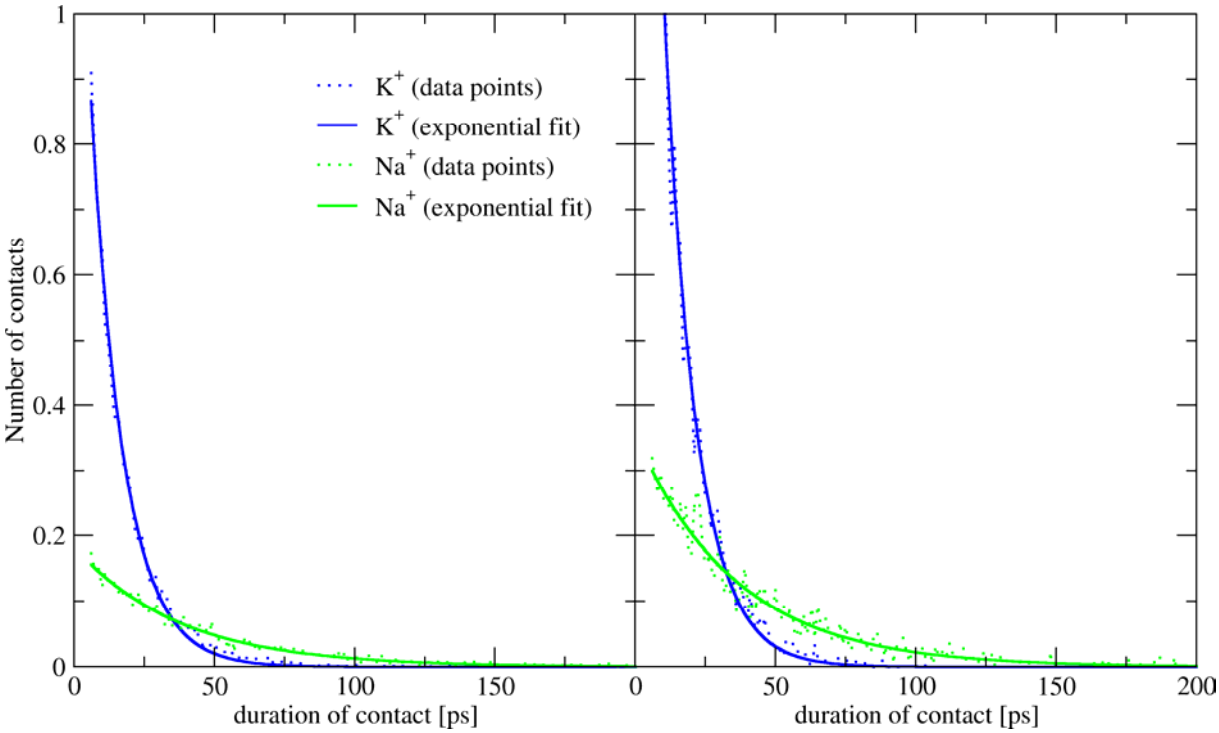
K+ (data points)
K+ (exponential fit)
Na+ (data points)
Na+ (exponential fit)
Number of contacts
duration of contact [ps]
duration of contact [ps]
0
0.2
0.4
0.6
0.8
1
0
50
100
150
200

**Figure 4**

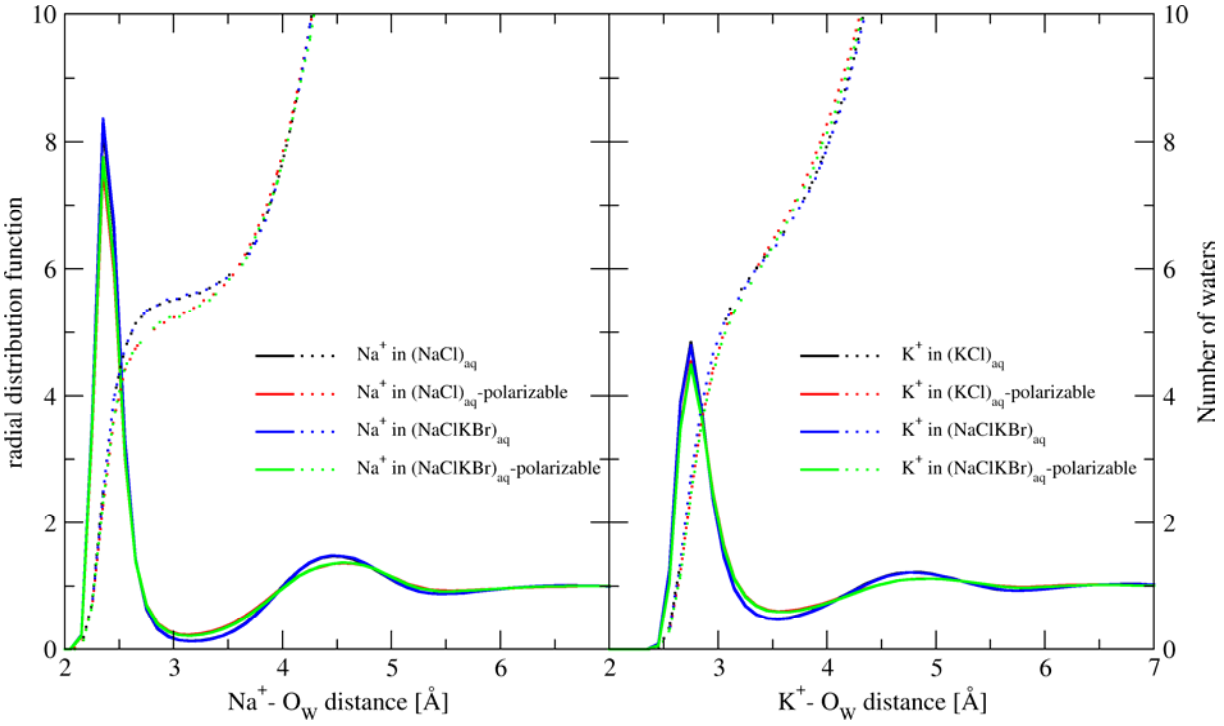
radial distribution function
Number of waters
Na+ in (NaCl)aq
Na+ in (NaCl)aq-polarizable
Na+ in (NaClKBr)aq
Na+ in (NaClKBr)aq-polarizable
Na+- Ow distance [Å]
K+ in (KCl)aq
K+ in (KCl)aq-polarizable
K+ in (NaClKBr)aq
K+ in (NaClKBr)aq-polarizable
K+- Ow distance [Å]

**Figure 5**

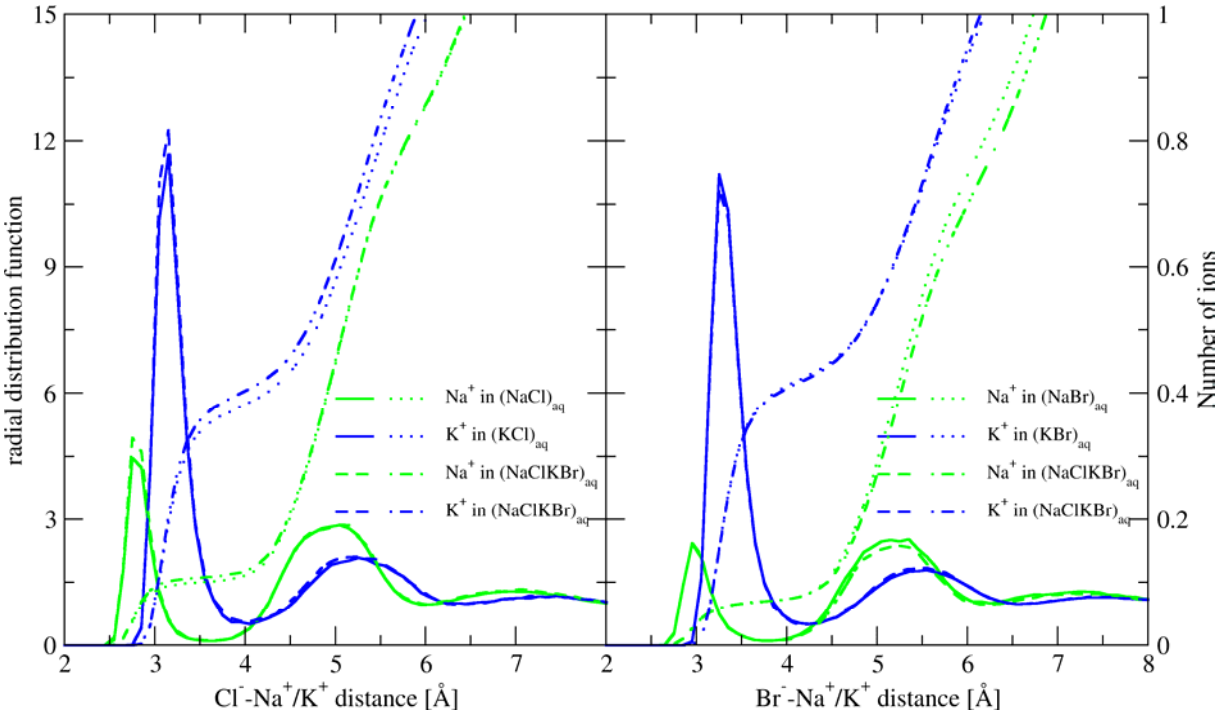
radial distribution function
Number of ions
Cl⁻-Na⁺/K⁺ distance [Å]
Br⁻-Na⁺/K⁺ distance [Å]
Na⁺ in (NaCl)aq
K⁺ in (KCl)aq
Na⁺ in (NaClKBr)aq
K⁺ in (NaClKBr)aq
Na⁺ in (NaBr)aq
K⁺ in (KBr)aq
Na⁺ in (NaClKBr)aq
K⁺ in (NaClKBr)aq

**Figure 6**

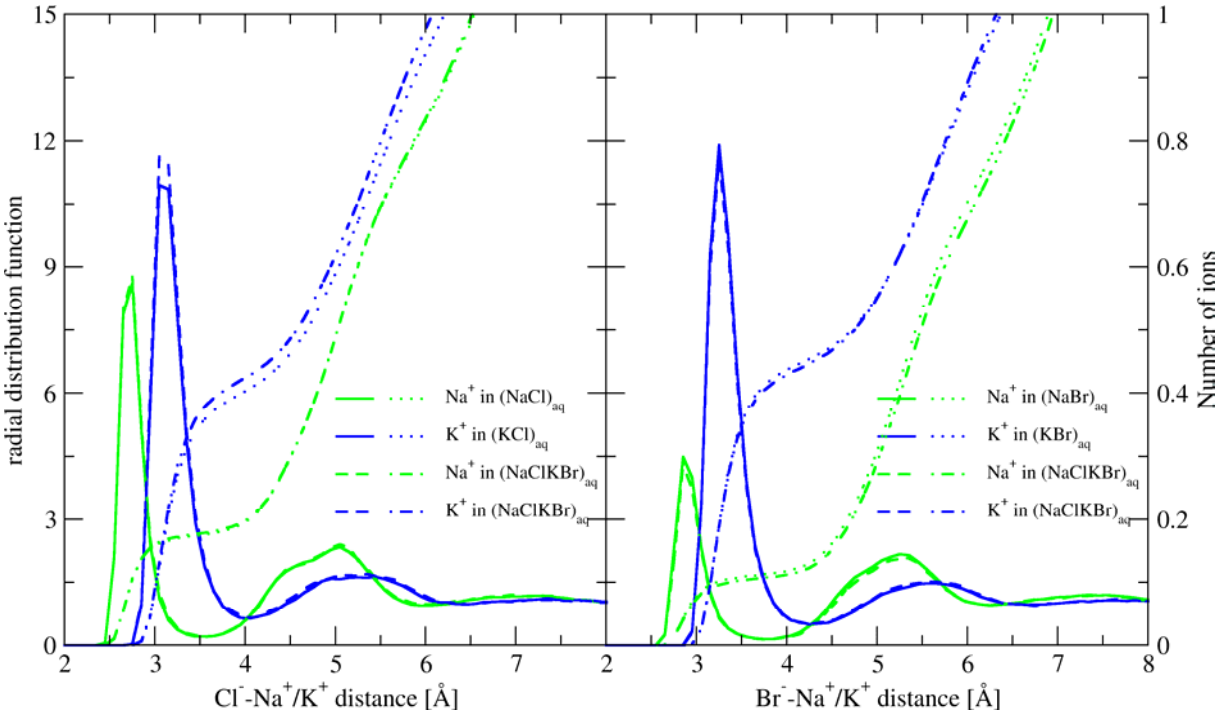
radial distribution function
Number of ions
Cl⁻-Na⁺/K⁺ distance [Å]
Br⁻-Na⁺/K⁺ distance [Å]
Na⁺ in (NaCl)aq
K⁺ in (KCl)aq
Na⁺ in (NaClKBr)aq
K⁺ in (NaClKBr)aq
Na⁺ in (NaBr)aq
K⁺ in (KBr)aq
Na⁺ in (NaClKBr)aq
K⁺ in (NaClKBr)aq

**Figure 7**

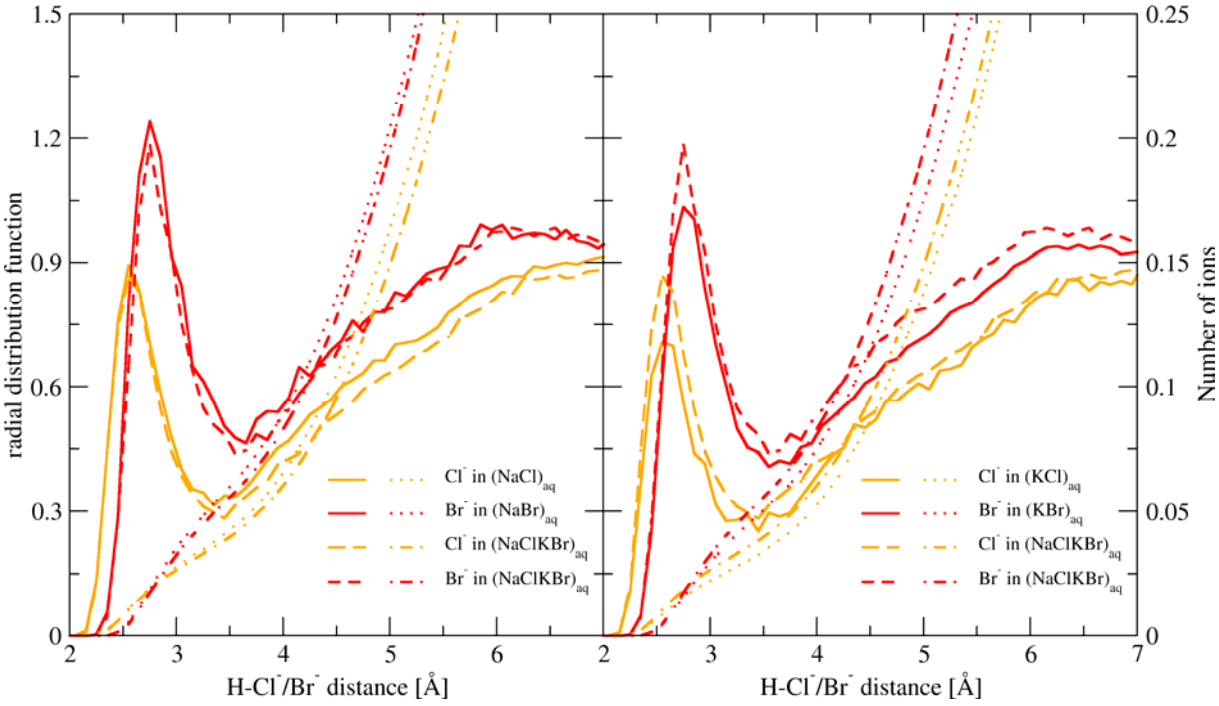
radial distribution function
Number of ions
H-Cl⁻/Br⁻ distance [Å]
H-Cl⁻/Br⁻ distance [Å]
Cl⁻ in (NaCl)aq
Br⁻ in (NaBr)aq
Cl⁻ in (NaClKBr)aq
Br⁻ in (NaClKBr)aq
Cl⁻ in (KCl)aq
Br⁻ in (KBr)aq
Cl⁻ in (NaClKBr)aq
Br⁻ in (NaClKBr)aq

**Figure 8**

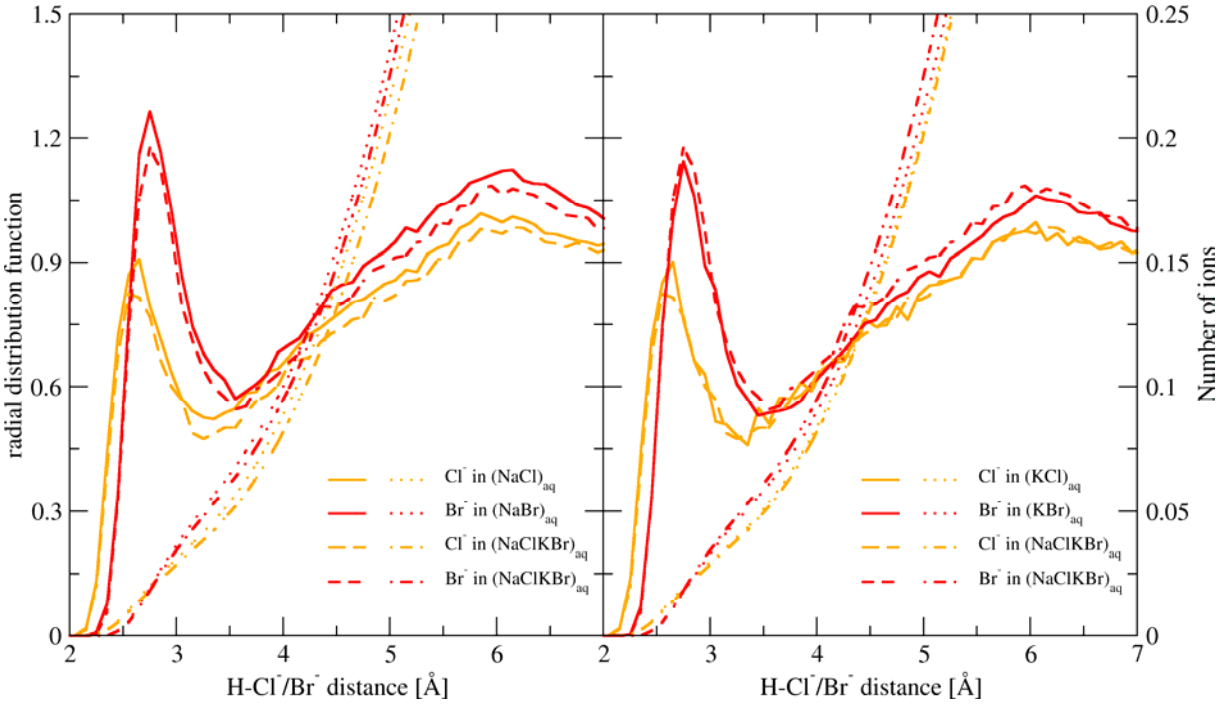
radial distribution function
Number of ions
H-Cl⁻/Br⁻ distance [Å]
H-Cl⁻/Br⁻ distance [Å]
Cl⁻ in (NaCl)aq
Br⁻ in (NaBr)aq
Cl⁻ in (NaClKBr)aq
Br⁻ in (NaClKBr)aq
Cl⁻ in (KCl)aq
Br⁻ in (KBr)aq
Cl⁻ in (NaClKBr)aq
Br⁻ in (NaClKBr)aq

**Figure 9**

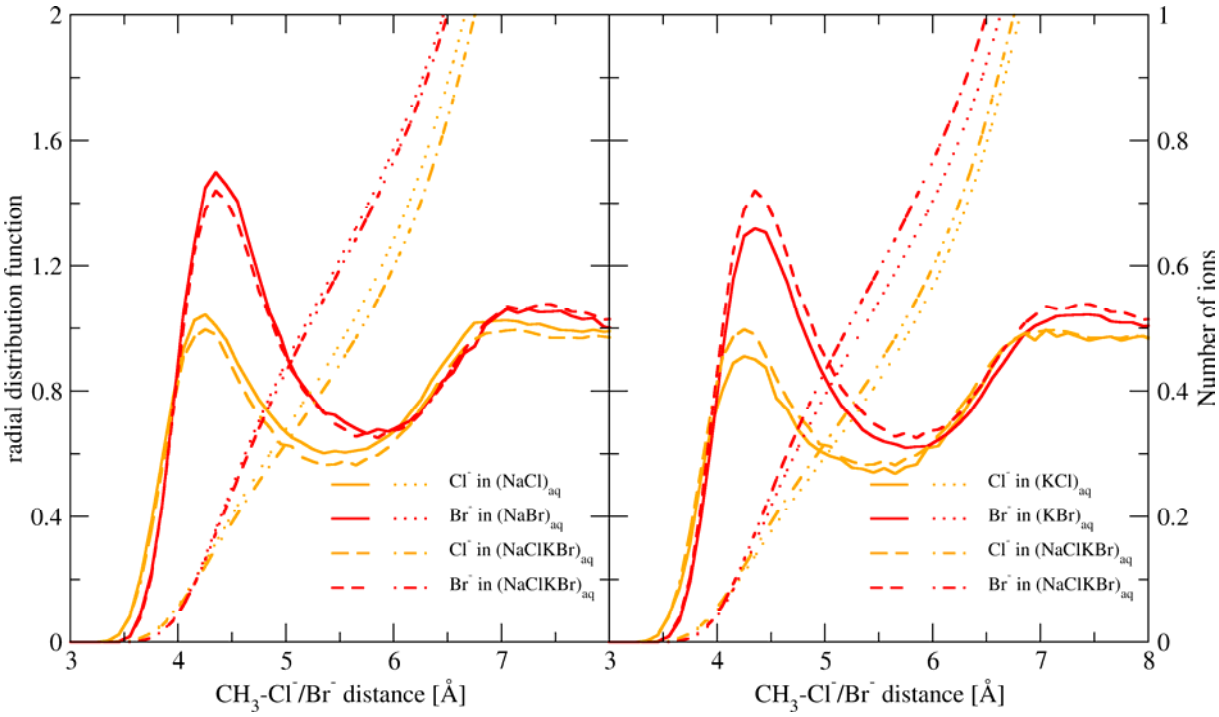
radial distribution function
Number of ions
CH3-Cl-/Br- distance [Å]
CH3-Cl-/Br- distance [Å]
Cl- in (NaCl)aq
Br- in (NaBr)aq
Cl- in (NaClKBr)aq
Br- in (NaClKBr)aq
Cl- in (KCl)aq
Br- in (KBr)aq
Cl- in (NaClKBr)aq
Br- in (NaClKBr)aq

**Figure 10**

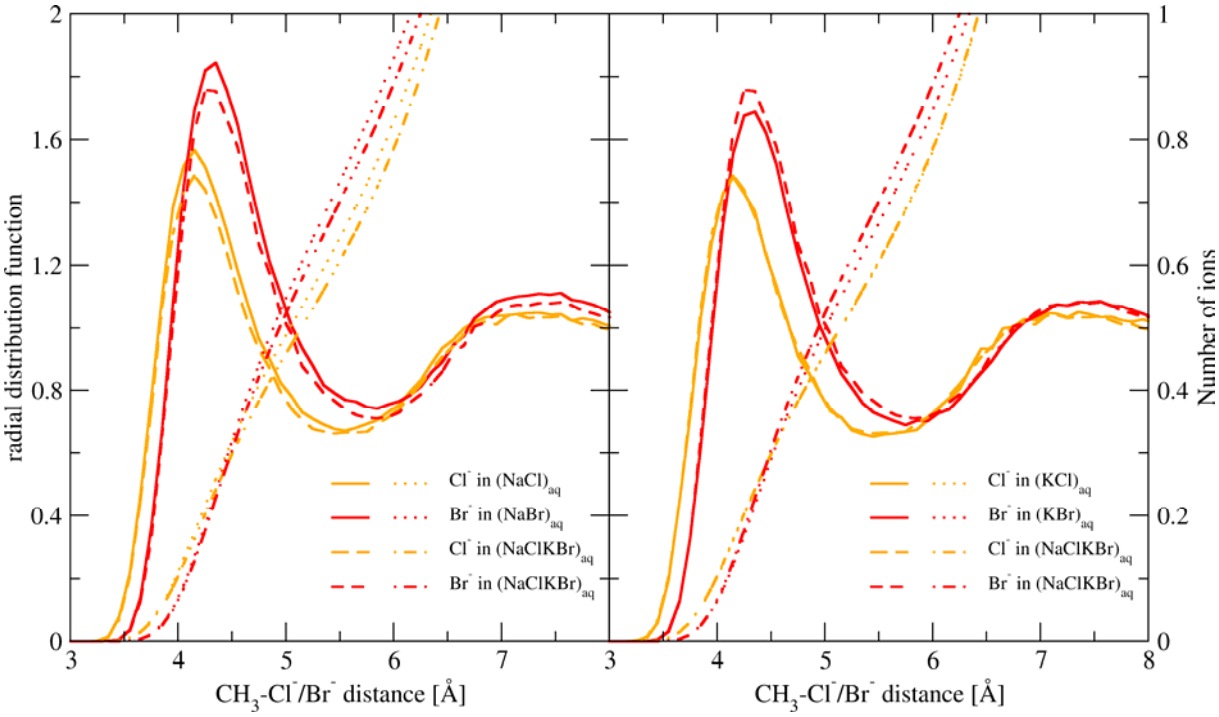
radial distribution function
Number of ions
CH3-Cl-/Br- distance [Å]
CH3-Cl-/Br- distance [Å]
Cl- in (NaCl)aq
Br- in (NaBr)aq
Cl- in (NaClKBr)aq
Br- in (NaClKBr)aq
Cl- in (KCl)aq
Br- in (KBr)aq
Cl- in (NaClKBr)aq
Br- in (NaClKBr)aq

**Figure 11**

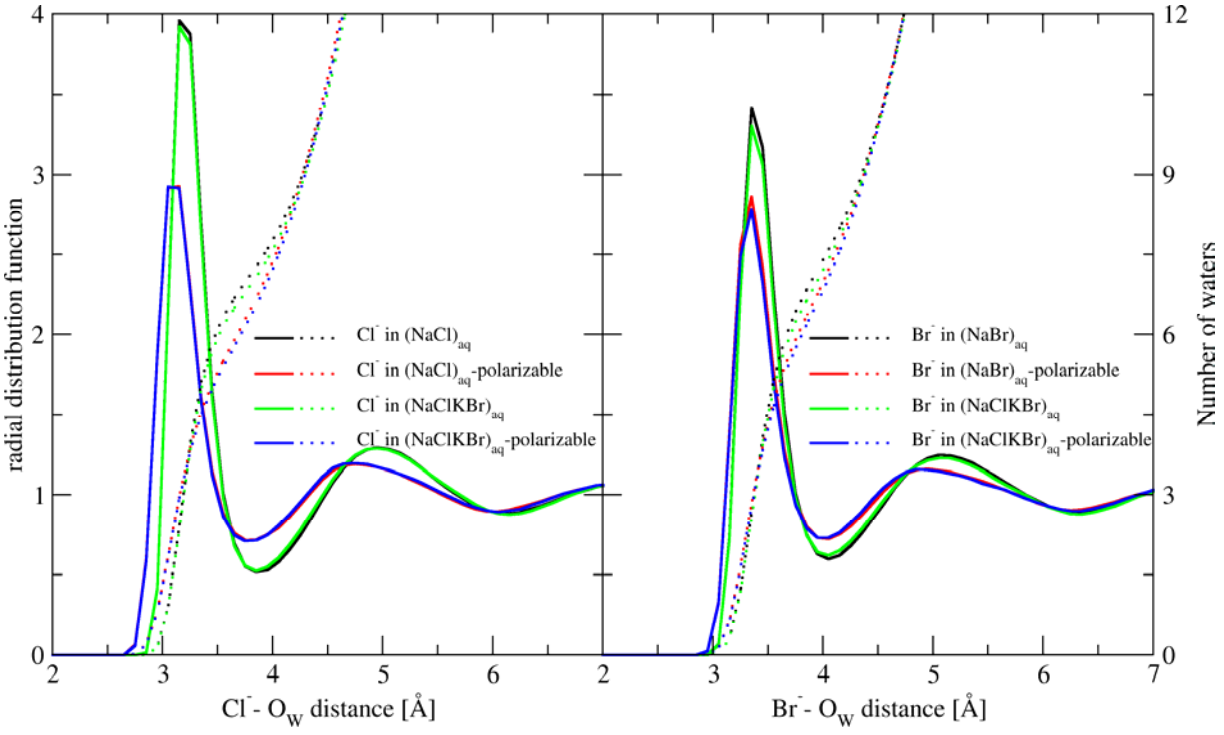
radial distribution function
Number of waters
Cl⁻ in (NaCl)aq
Cl⁻ in (NaCl)aq-polarizable
Cl⁻ in (NaClKBr)aq
Cl⁻ in (NaClKBr)aq-polarizable
Cl⁻ - OW distance [Å]
Br⁻ in (NaBr)aq
Br⁻ in (NaBr)aq-polarizable
Br⁻ in (NaClKBr)aq
Br⁻ in (NaClKBr)aq-polarizable
Br⁻ - OW distance [Å]

**Figure 12**

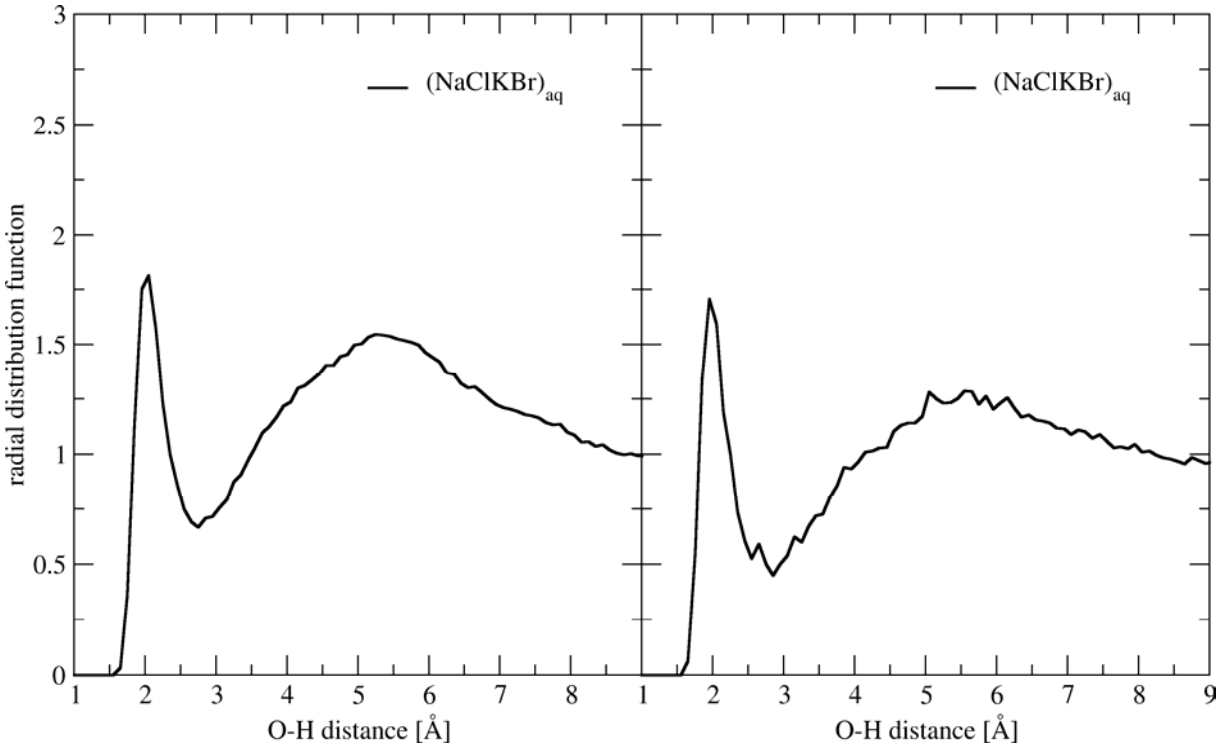
radial distribution function
(NaClKBr)aq
(NaClKBr)aq
O-H distance [Å]
O-H distance [Å]

**Figure 13**

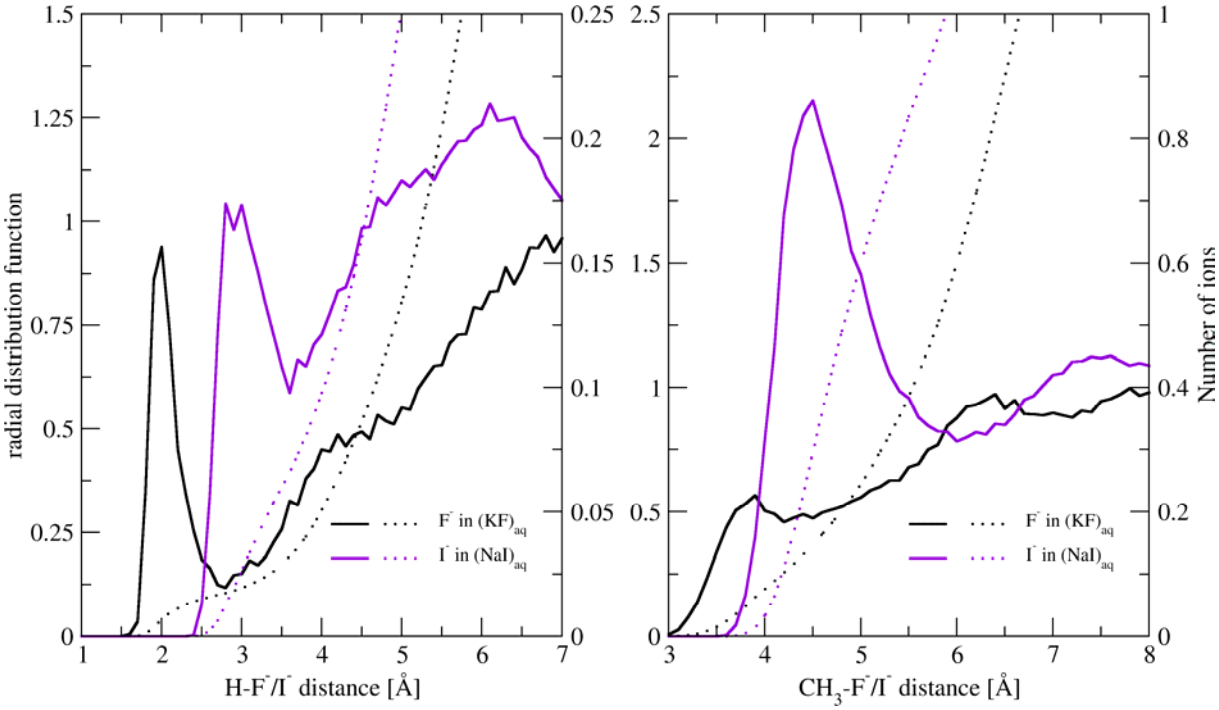
radial distribution function
Number of ions
H-F⁻/I⁻ distance [Å]
CH3-F⁻/I⁻ distance [Å]
F⁻ in (KF)aq
I⁻ in (NaI)aq

**Figure 14**

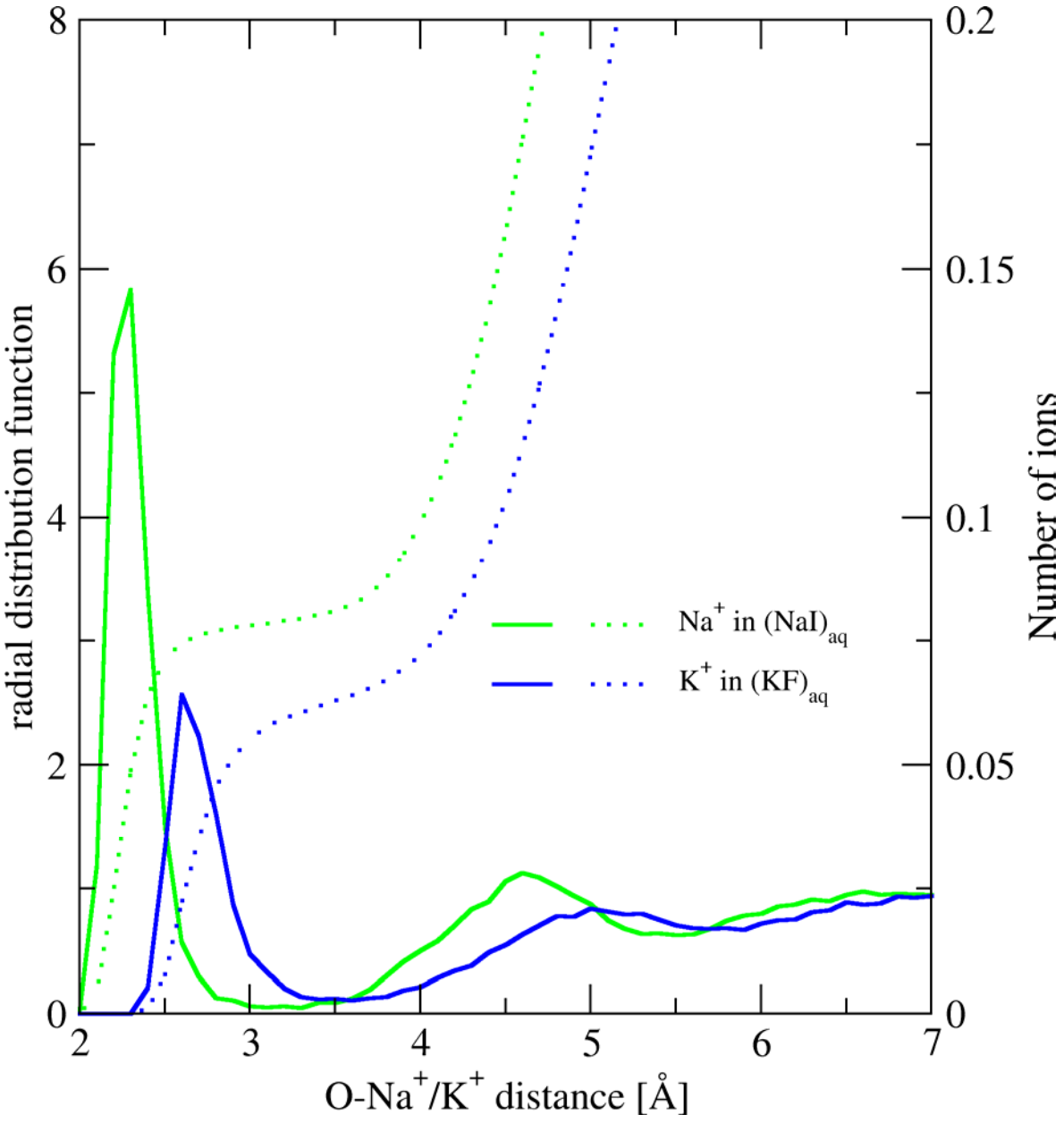
radial distribution function
Number of ions
O-Na+/K+ distance [Å]
Na+ in (NaI)aq
K+ in (KF)aq
0
2
4
6
8
0
0.05
0.1
0.15
0.2
2
3
4
5
6
7

**Figure 15**

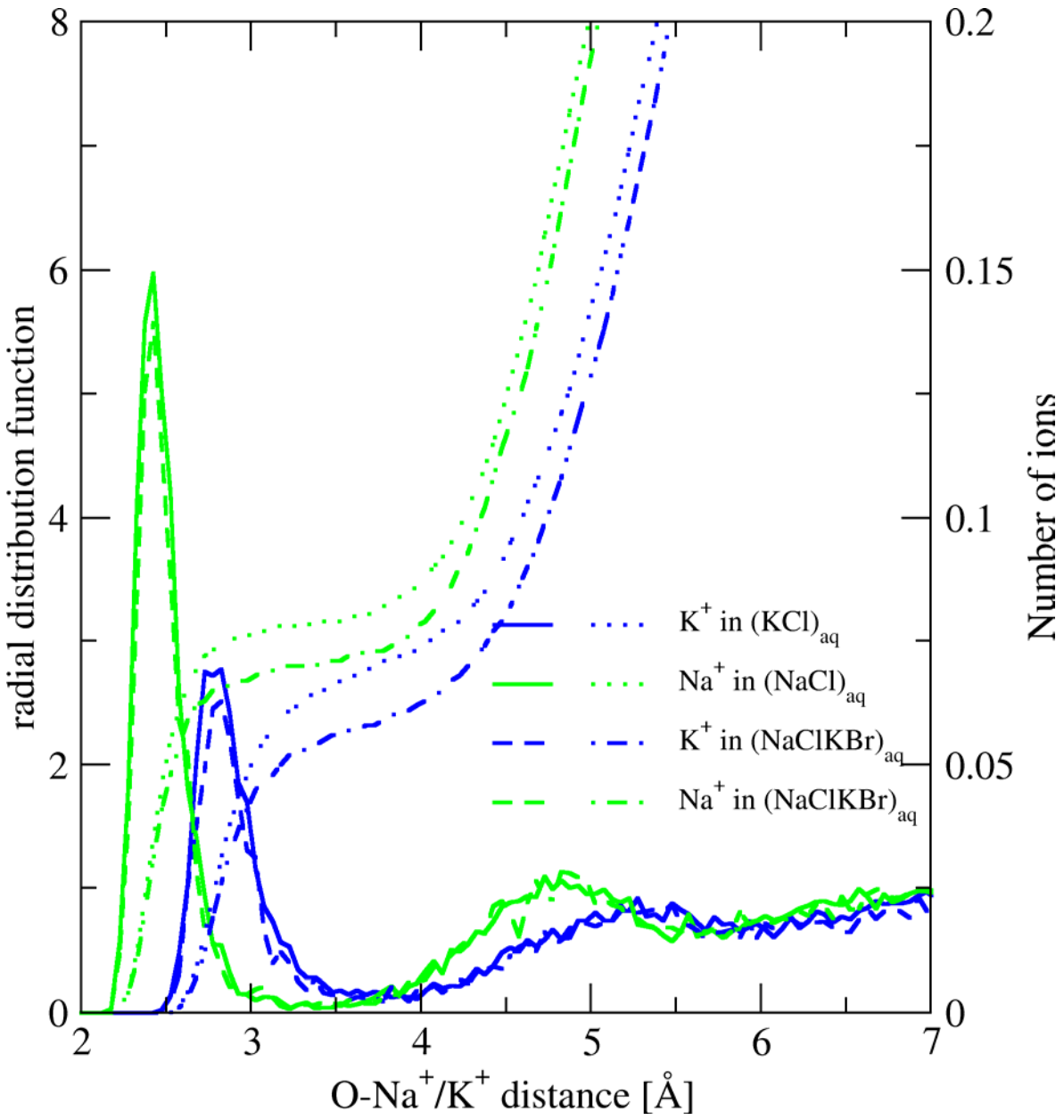
radial distribution function
Number of ions
O-Na+/K+ distance [Å]
K+ in (KCl)aq
Na+ in (NaCl)aq
K+ in (NaClKBr)aq
Na+ in (NaClKBr)aq
0
2
4
6
8
0
0.05
0.1
0.15
0.2
2
3
4
5
6
7

**TOC Graphics**

Distributions of sodium (green) and potassium (blue) around aqueous N-methylacetamide.